

A Determination and Analysis of the Thermionic Constants of Thoriated Tungsten

ALBERT ROSE, *Cornell University**

(Received March 2, 1936)

The slopes and intercepts of Richardson plots are obtained for states of activation from a flashed to a completely thoriated surface, and for applied fields up to 3×10^4 volts/cm. The following observations are described: (1) abnormal decrease of work function with low applied fields, (2) effect of bombardment with positive ions, (3) effect of aging at high temperatures, (4) proportionality of the log of the intercept and the slope at a given state of activation, (5) variation of the low field intercept of the Richardson plot with activation, (6) variation of the high field intercept of the Richardson plot with activation,

(7) (8) emission lag effects at high and low applied fields (9) dependence on temperature of the anomalous Schottky effect. The observations are analyzed in terms of an assumed patch distribution of adsorbed atoms such that the concentration difference between patches decreases with increasing temperature. More complete information is presented concerning the temperature coefficients of the work function for thoriated tungsten, and the precautions necessary before comparisons are made with temperature coefficients obtained photoelectrically or by contact potential measurements.

INTRODUCTION

THE reported values of the thermionic constants of thoriated tungsten, namely, the slope and intercept of the Richardson plot, show a divergence larger than the experimental errors of the individual values. Reimann¹ gives the extent of this divergence for the reported values of the intercept as a function of activation. The reported slopes disagree by several tenths of a volt. Experimentally, Brattain and Becker² have shown why this lack of agreement is to be expected. For any given state of activation the slope and intercept decrease markedly with applied field, in the range of applied fields generally used. The over-all change of intercept is of the order of a factor 10, and the over-all change of slope of the order of 0.5 volt. For any given state of activation, therefore, depending upon the applied field, the reported values of the slope and intercept might be expected to differ by as much as these amounts.

The rapid decrease of the slope of the Richardson plot with applied field, which, in terms of the current-voltage curve, has been long familiar as the anomalous Schottky effect, has been successfully analyzed in terms of the patch theory.^{3, 4} The rapid decrease of intercept with applied field may also be accounted for by the patch theory if it is assumed that the concentration

difference between patches decreases with increasing temperature.⁵ This analysis is undertaken below. For the purpose of the analysis, it was necessary to make a more thorough study of the dependence of the thermionic constants for thoriated tungsten on activation and applied field than was reported in the paper by Brattain and Becker. These results, also, are summarized below.

EXPERIMENTAL ARRANGEMENT

The tube consisted essentially of a one-mil thoriated tungsten filament, 6 cm long, mounted along the axis of a cylindrical collector, and two guard rings. The filament was a "long" filament down to 1200°K as shown both by the unbroken Richardson lines in this temperature range and by calculations based on the paper by Langmuir, McLane and Blodgett.⁶ This allowed the current-temperature scale of the Jones and Langmuir⁷ tables to be applied directly. The vacuum was 10^{-7} mm of Hg or better as read by an ionization gauge. Two significant tests of the vacuum conditions were first, that emission values could be repeated over a period of several weeks and second, that no appreciable sputtering of the thorium occurred at 300 volts applied collecting voltage. These tests are an adequate measure of the presence of chemically active and inert gases.

* Now employed by RCA Manufacturing Co., Radio-tron Division, Harrison, New Jersey.

¹ A. L. Reimann, *Thermionic Emission*, page 127.

² Brattain and Becker, *Phys. Rev.* **43**, 428 (1933).

³ J. A. Becker, *Rev. Mod. Phys.* **7**, 95 (1935).

⁴ A. Rose, *Phys. Rev.* **47**, 806 (1935).

⁵ A. Rose, *Phys. Rev.* **47**, 889 (1935).

⁶ Langmuir, McLane and Blodgett, *Phys. Rev.* **35**, 478 (1935).

⁷ Jones and Langmuir, *Gen. Elec. Rev.*, pp. 310-319, 354-361, 408-412 (1927).

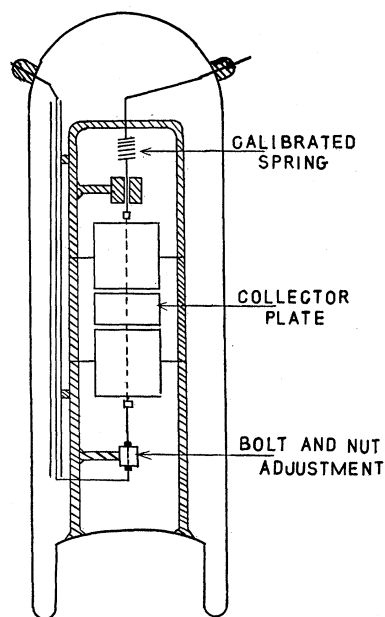


FIG. 1. Experimental tube. The calibrated spring and adjustment at the lower end were necessary to accurately fix the filament tension to prevent sagging and burning out at the higher temperatures.

RESULTS

The emission current was measured as a function of the three variables, temperature, T , applied field, E , and activation, f , in the ranges:

$$1300^{\circ}\text{K} < T < 1800^{\circ}\text{K}$$

$$0 < E < 3 \times 10^4 \text{ volts/cm}$$

$$0 < f < 1.$$

The f values were based upon tables given by Brattain and Becker² in the paper cited above. Although the f value does not uniquely characterize the surface, because of its patchy nature, it is a convenient index to the concentration of thorium atoms in the more concentrated patches. The results are summarized by the curves in Figs. 2 and 3 showing the observed slopes and intercepts of the Richardson plots ($\ln I - 2 \ln T$ against $1/T$) as a function of applied voltage for various states of activation. The field at the surface of the filament in volts/cm calculated from the geometry of the elements was 117 times the applied voltage. A similar set of data was taken after the filament had been aged several hours at 3000°K. These curves differed

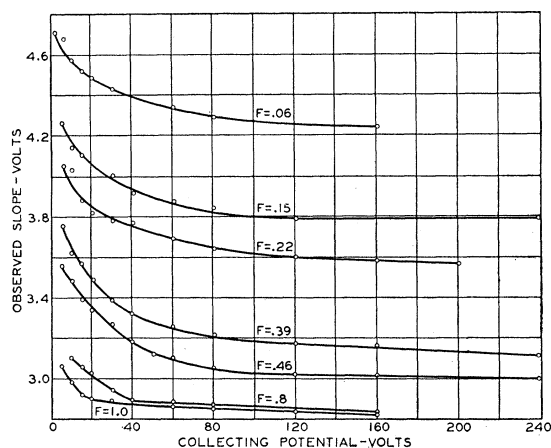


FIG. 2. Slopes of Richardson plots as a function of collecting potential for various states of activation. The field (volts/cm) at the surface of the filament = 117 × collecting potential.

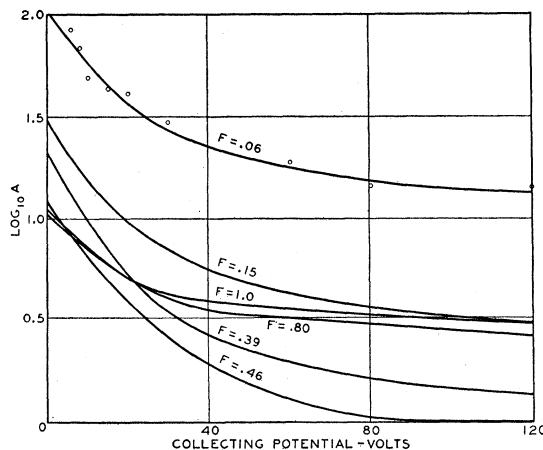


FIG. 3. Log of the intercepts of Richardson plots as a function of collecting voltage for various states of activation.

from the set shown here in that they flattened out at lower collecting voltages.

DISCUSSION OF RESULTS

Because of the patch distribution of adsorbed atoms on the surface, and the consequent dependence of the thermionic constants on the particular surface investigated, the absolute magnitudes of the constants are not to be emphasized. What should be emphasized is the variation of these constants with activation and applied field. This is characteristic of all thoriated tungsten surfaces and, therefore, requires an

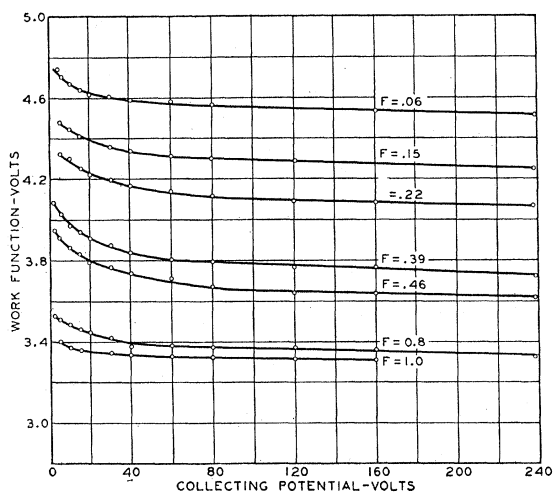


FIG. 4. Work functions (obtained from the slopes and intercepts of Richardson plots) as a function of collecting potential for various states of activation.

explanation. The major facts concerning this variation are enumerated below.

(1) The most prominent characteristic is the marked decrease of the work function⁸ with applied field for low applied fields. The curves (Fig. 4) flatten out at around 10^4 volts/cm. This is the counterpart of the poor saturation observed for all coated surfaces, namely, a more rapid decrease of the work function with applied field than is predicted by the normal Schottky effect.

(2) The rate of decrease of the work function with applied field is accentuated by bombardment of the thoriated surface with positive ions. (See Fig. 5.)

(3) The curves for work function against applied field flatten out at lower applied fields after the filament has been aged at high temperatures.

(4) Within the accuracy of measurement of the intercept of the Richardson plot, and for applied fields below the point where the curves flatten out, the change of the log of the intercept is proportional to the change of the slope at a given state of activation. (See Fig. 6.) It is to be remembered that at a given state of activation the slope and the intercept are both a function of the applied field. (This is not to be confused with the reported proportionality between the slope and intercept for different states of activation and the same applied field.)

(5) The intercept of the Richardson plot for low applied fields decreases steadily with activation to a minimum at complete activation.

(6) The intercept of the Richardson plot at high applied fields (in the neighborhood of the point where the curves in Fig. 4 flatten out) decreases with activation to a minimum around *half* activation. (See Fig. 7.) This is borne out also by the results of Brattain and Becker, which show

⁸ The work function as indicated below in Eq. (5) is obtained from the slope and intercept of the Richardson plot.

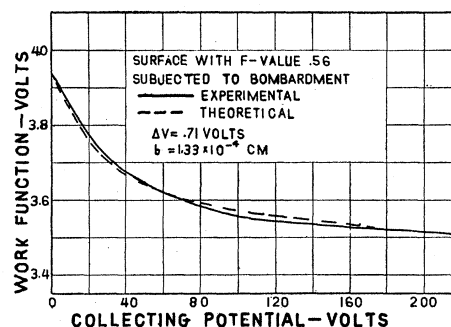


FIG. 5. Effect of positive-ion bombardment on the surface of a partially activated thoriated tungsten filament. The enhanced over-all change in work function with applied potential is the well-known anomalous Schottky effect. (b = length of side of square patch.)

the intercept against applied field for $f=0.6$ intersecting similar curves for $f=0.86$ and $f=1.0$.

(7) At high applied fields, when the temperature of a partially activated filament is suddenly dropped from about 1600°K to about 1300°K , the emission increases (by as much as a factor of two) with time at this lower temperature approaching asymptotically a reproducible value. If the temperature is now suddenly increased to 1600°K , no time lag in the emission is observed within the 7-second period of the galvanometer.

(8) At low applied fields, when the filament temperature is suddenly dropped to a low value, the emission at this lower temperature decreases only *slightly* with time or may even be constant.⁹

ANALYSIS OF RESULTS

It is the purpose of this part to analyze the facts enumerated above on the basis of a patch distribution of adsorbed atoms such that the concentration difference between patches decreases with increasing temperature. The patch distribution is well established by electron microscope pictures of activated surfaces. The temperature dependence is a natural assumption by Boltzmann's distribution function, if the adsorption energy of neighboring patches is different.

To carry out the analysis, certain simplifying assumptions must be made since an exact treatment is both out of the question and not in keeping with the experimental uncertainties. It is hoped that these assumptions will be within the range of experimental variations due to the patches, or, at least, faithful to the more important elements of the problem. In particular, use

⁹ I am indebted to Dr. Nottingham for this fact.

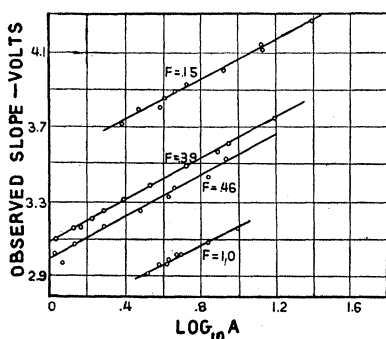


FIG. 6. Linear relation between observed slopes and intercepts of Richardson plots for several states of activation.

will be made of the fact that about ten or twenty times as much emission comes from the low work function patches as from the high work function patches. And since the low work function patches dominate the variation of the observed constants with activation and applied field, the approximation will be made that they are entirely responsible for the observed variation. This is especially true, since, as will appear below, the rapid variation of the constants is due to the local retarding patch field above the low work function patches. The local patch field above the high work function patches is an accelerating field, and changes in it introduce only the relatively small *normal* Schottky correction. Other approximations will be explained as they are introduced.

For the purpose of the analysis, a more explicit form of the Richardson equation, based upon three assumptions, is employed. These assumptions are:

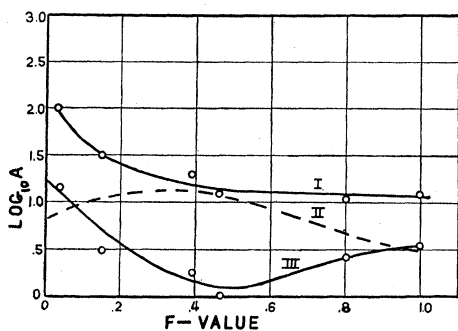


FIG. 7. Curve I: log of the low applied field intercept: $\log U - (\epsilon/2.3k)(\alpha_1 + \alpha_2)$. Curve III: log of the high applied field intercept: $\log U - (\epsilon/2.3k)(\alpha_1 + \alpha_2 + \alpha_3)$. Curve II: $(\epsilon/2.3k)\alpha_3$.

(1) The validity of the statistical form of the Richardson equation

$$I = UT^2 e^{-\epsilon\phi/kT},$$

where U = universal constant 120 amp./cm²/°K²,

T = absolute temperature,

ϕ = work function,

ϵ, k have their usual significance.

(2) The work function ϕ is a function of applied field and temperature

$$\phi = \phi(E, T).$$

(3) $\partial^n \phi / \partial T^n = 0$ for $n > 1$.

(1) is based upon the Fermi distribution for electrons in metals; (2) is an experimental fact; and (3) merely states that only Richardson plots which are straight lines will be considered. This last is a valid restriction since the Richardson plots even for coated surfaces are indistinguishable from straight lines in the experimental range of temperatures.

If $\phi(E, T)$ is expanded in a Taylor series in the neighborhood of (E_1, T_1) in the experimental range of applied field and temperature and the terms grouped together with due regard to (3), the result will take the form:

$$\phi(E, T) = \phi_0 + \alpha T + \beta(E)T + \gamma(E), \quad (1)$$

where $\beta(E)$ and $\gamma(E)$ may be any functions of the applied field and ϕ_0 and α are constants. The Richardson equation now becomes:

$$I = U e^{-(\epsilon/k)[\alpha + \beta(E)]} T^2 e^{-(\epsilon/k)[\phi_0 + \gamma(E)]} / T, \quad (2)$$

where $U e^{-(\epsilon/k)[\alpha + \beta(E)]}$ (3)

is the observed intercept.¹⁰

$$(\epsilon/k)[\phi_0 + \gamma(E)] \quad (4)$$

is the observed slope and

$$\phi_0 + \gamma(E) + [\alpha + \beta(E)]T \quad (5)$$

is the work function at temperature T and applied field E .

The eight experimental observations enumerated in the previous section may now be examined in order.

¹⁰ In the case of patch distributions, the intercept should also contain a surface factor $e^{\phi(E)}$ to take care of the fact that at higher fields more of the emission comes from the low work function patches, that is, the effective emitting area decreases. This effect, however, is small compared with the change of intercept actually observed (see appendix).

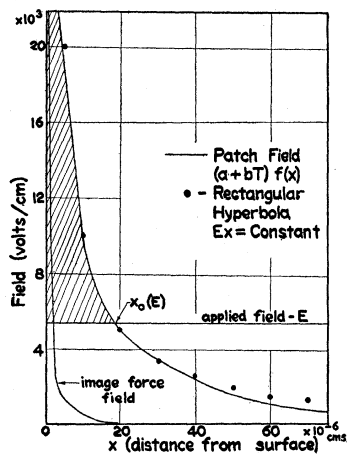


FIG. 8. The above figure shows: (1) The relative unimportance of the image force field as compared with the patch field $(a+bT)f(x)$. (2) The increase in work function (shaded area) of the low work function patch due to the retarding patch field at an applied collecting field E . (3) The approximation of the patch field by a rectangular hyperbola.

1.

The curves in Fig. 2 must be corrected by the intercept, according to (5), to get the actual work function at a given applied field and temperature. Fig. 4 shows the variation of work function, so obtained, with applied field for several states of activation. The temperature chosen was 1600°K. The abnormal decrease of work function for low applied fields is due to the local retarding field above the low work function patch. These local fields were calculated for a checker-board array of patches. The adjustable parameters are ΔV , the contact potential difference (or difference in work function) between the two kinds of patches, and s the length of side of each square patch. (See appendix for mathematical detail.) Knowing the local fields due to the patches and the applied field, the work function may be calculated for each point on the surface and averaged over the whole surface to give the observed value.

A typical comparison of calculated and observed work function against applied field curves is shown in Fig. 9. The agreement is as close as can be expected from the arbitrary assumed distribution of patches. Where the curves flatten out, the applied field becomes equal to the patch field at the surface. Beyond this point the variation of work function with applied field is practically that predicted by the normal Schottky

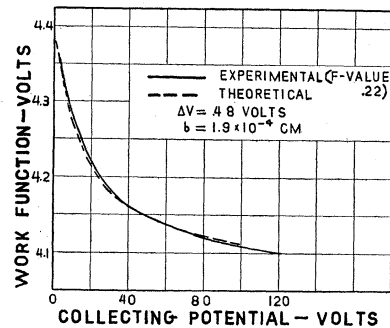


FIG. 9. Agreement between calculated and observed variation of work function with applied field. Calculations were made on the basis of a square array patch theory. (b = length of side of square patch.)

effect, and the calculated curve, which neglects the normal Schottky effect, is not valid.

The parameters s and ΔV were obtained for states of activation from $f=0$ to $f=1$ and recorded in Table I. It is to be noted that the ΔV values are well within the contact potential, about two volts, between clean and completely thoriated tungsten. The values of the average patch size are of the order of the size of crystal observed by an optical microscope for this filament. The quantitative comparison is made below in (2). In Table I are recorded, also, values of s and ΔV estimated from Brattain and Becker's data. The s values in their case are consistently larger than ours. Since, as is noted below in (2), the patch size is of the order of the exposed tungsten crystal faces, this difference is explainable. The patch size remains roughly constant with activation, as would be expected. The average contact potential between patches shows a maximum for states of activation around $f=0.5$ and decreases as $f \rightarrow 1$. The reason for this is that a given concentration difference corresponds to a larger difference in work function for the lower states of activation than for the higher ones. (The work function against activation curve drops rapidly in the range $f=0$ to $f=0.5$ and then flattens out to a broad minimum at $f=1$.)

2.

Also in Table I are recorded the values of s and ΔV obtained from a set of slope and intercept against applied field curves for various states of activation after the filament had been aged several hours at 3000°K. The values of s are

seen to be about twice as large as those recorded before the aging. This is in agreement with the fact that crystal growth is known to occur at this temperature.

While the method used here of estimating the average patch size is a reliable means of determining relative values, as in the comparison of the average patch size before and after aging, it is not to be expected that it will give more than the order of magnitude of the absolute values. In particular, the flattening out point of the work function against applied field curves is used to determine the value of the patch field at the surface, and this is likely to be determined by the higher patch fields of the smaller patches rather than by the field corresponding to the average sized patch. With this in mind, the comparison of the following optical observations on the exposed crystal faces of the filament with the s values of average patch size just cited will be significant. The optical microscope showed about 75 percent of the exposed crystal faces to be rectangles with their long side 3 or 4 times their short side, and lying parallel to the length of the filament. The short side, which would determine the patch field at the surface, was of the order of 6×10^{-4} cm. Further work with the electron microscope should show how meaningful the comparison between the 6×10^{-4} cm crystal dimension and the $3-4 \times 10^{-4}$ cm average patch size is. One further fact is brought out by the s values in the last column of Table I, namely, for low states of activation s is small. Electron microscope pictures at these states of activation

show a number of isolated spots smaller than the average patch size at higher activations.

3.

Fig. 5 shows the effect on the work function against applied field curve of bombarding the thoriated surface with positive ions. Under the action of the bombardment, thorium is sputtered off in spots, resulting in a larger difference in concentration between patches. This is brought out by the larger value of ΔV necessary to be assumed to match the calculated and observed curves.

4.

The fact that at a given state of activation the change of slope is proportional to the change of the log of the intercept (Fig. 6) (both being functions of the applied field) is a stringent condition to be satisfied by any theory of the thermionic constants for coated surfaces. The difficulty comes in trying to find a mechanism which will cause the intercept to decrease rapidly for low applied fields and yet have no effect at high applied fields. The explanation, several times offered, to account for changes in the intercept, namely, that the transmission coefficient varies with applied field, is immediately seen to be invalid here. The transmission coefficient explanation is most effective at high applied fields. Actually, however, the intercept decreases most rapidly for low applied fields and becomes constant at around 10^4 volts/cm. The temperature-dependent patch theory not only accounts for this rapid decrease at low fields but shows why the change of the log of the intercept is linked up with the change of slope and, in particular, why these changes are *proportional*.

The explanation is qualitatively this: the slope decreases rapidly with low applied fields because the local retarding patch field above the low work function patch is rapidly neutralized by the applied field. The intercept will change, according to Eq. (3), if the temperature coefficient of the work function is also a function of the applied field. This condition is provided by the temperature dependent patch theory in the following way: Since the local patch fields are proportional to the contact potential difference between patches, and since this changes with temperature

TABLE I. Parameters s and ΔV for various states of activation. Values of ΔV (average contact potential difference between patches) and s (average size of patch computed on the basis of the square array patch theory) were computed from work function against applied field curves at various states of activation.

			AFTER AGING 2 HOURS AT 3000°K			COMPUTED FROM BRAT- TAIN AND BECKER'S DATA ON A 4-MIL THORIATED TUNG- STEN FILAMENT		
f VAL- UE	ΔV (volts)	s (cm)	f VAL- UE	ΔV (volts)	s (cm)	f VAL- UE	ΔV (volts)	s (cm)
0.06	0.46	1.5×10^{-4}	0.08	0.36	1.5×10^{-4}	0.3	0.8	4.6×10^{-4}
.15	.50	1.6	.27	.46	2.8	.6	.70	2.8*
.22	.60	1.7	.57	.46	3.8	.86	.34	4.6
.39	.68	1.9	.76	.48	4.0	1.0	.30	5.4
.46	.70	2.0	.87	.38	3.2			
.8	.36	2.0	1.0	.22	3.7			
1.0	.24	1.2						

* Data incomplete.

due to the decrease of concentration difference with increasing temperature, then the local retarding field above the low work function patch must also change with temperature. Corresponding to this change there will be a temperature coefficient of the work function which will depend upon the applied field in the same way as the slope, since it will be proportional to the amount of retarding field not neutralized by the applied field. In other words, a given change of retarding field with temperature has its maximum effect on the work function when the applied field is zero. When the applied field completely neutralizes the retarding field, changes in the retarding field with temperature have no effect upon the work function. Hence, the intercept at these fields remains constant.

To make the argument more definite: (1) Let the contact potential between patches be

$$\Delta V = a + bT^{11}$$

where a and b are constants. (2) Let all of the emission come from the low work function patches. According to Eqs. (3) and (4), this proof must show that:

$$d\beta(E)/dE \sim d\gamma(E)/dE.$$

At any applied field E , the contribution of the patch field to the work function is (see Fig. 8):

$$\begin{aligned} \beta(E)T + \gamma(E) &= \int_0^{X_0(E)} [(a+bT)f(X) - E]dX \\ &= -EX_0(E) + (a+bT) \int_0^{X_0(E)} f(X)dX, \quad (6) \end{aligned}$$

where $(a+bT)f(X)^{12}$ is the retarding patch field as a function of X , the distance from the surface;

¹¹ The contact potential undoubtedly contains higher powers of T , but these may be neglected, as long as the Richardson plots are indistinguishable from straight lines.

¹² As may be seen from Fig. 8, the image force field may be neglected in comparison with the patch field up to a short distance from the surface about 5×10^{-6} cm. (Although for large values of X , the image field must be larger than the patch field, since the image field decreases as $1/X^2$ and the patch field as $e^{-\text{const.} X}$, the values of E for which this is true are so small that an applied potential of one volt already brings $X_0(E)$ in the range shown in Fig. 8.) However, for applied fields that bring $X_0(E)$ within this distance 5×10^{-6} cm the proportionality between the log of the intercept and the slope no longer holds experimentally so that this analysis may be restricted to the range of $X_0(E)$ for which the patch field is much greater than the image field.

$X_0(E)^{13}$ is the distance from the surface at which the applied field equals the retarding field.

$$\begin{aligned} \beta(E) &= \frac{\partial}{\partial T} \left[-EX_0(E) + (a+bT) \int_0^{X_0(E)} f(X)dX \right] \\ &= b \int_0^{X_0(E)} f(X)dX, \end{aligned}$$

$$\gamma(E) = -EX_0(E) + a \int_0^{X_0(E)} f(X)dX.$$

It is evident by inspection of $\beta(E)$ and $\gamma(E)$ that $d\beta(E)/dE = \text{const.} X d\gamma(E)/dE$ if

$$\begin{aligned} (d/dE)[EX_0(E)] \\ = 0 \text{ or const. } X(d/dE) \int_0^{X_0(E)} f(X)dX. \end{aligned}$$

The former possibility is nearly satisfied, since the form of the surface field $f(X)$ is, in the important part of its range, nearly that of a rectangular hyperbola for which $(d/dE)[EX_0(E)] = 0$. This is evident from Fig. 8 in which a rectangular hyperbola is matched with the retarding field $(a+bT)f(X)$ computed along a normal to the center of a low work function patch. Hence, within the limits of experimental error, the temperature dependent patch theory accounts for the significant straight lines in Fig. 6.

5 and 6.

Fig. 7 shows that the low field intercept decreases with activation to a minimum near complete activation. The high field intercept, on the other hand, shows a minimum around $f=0.5$. The following is a qualitative analysis to explain the difference by the temperature dependent patch theory.

In general the intercept is

$$Ue^{-(\epsilon/k)[\alpha + \beta(E)]}.$$

The $\beta(E)$ has been identified with the change of the local fields with temperature due to the decrease of the concentration difference between patches. The α term may be split into three

¹³ $X_0(E)$ is also a function of T , but its dependence on T is of the order of the dependence of the slopes of the Richardson plots on T , which has been neglected as long as these are indistinguishable from straight lines.

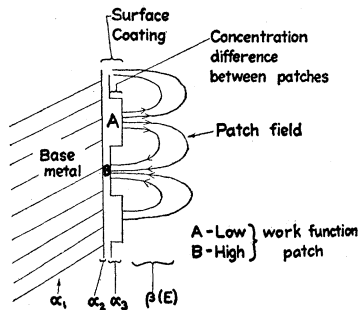


FIG. 10. Schematic representation of the various causes for a temperature coefficient of the work function: α_1 —base metal—change of Fermi limit. α_2 —uniform adsorbed layer of atoms. e.g. A surface uniformly covered with an adsorbed layer shows a temperature coefficient different from α_1 . α_3 —concentration difference between the two kinds of patches. This concentration difference decreases with increasing temperature. $B(E)$ —retarding patch field above the low work function patches. This retarding field decreases with decreasing concentration difference, i.e., with increasing temperature.

parts: α_1 associated with the base metal, α_2 associated with the temperature change of the dipole moment per adsorbed atom, and α_3 with the temperature change of concentration of the patches (see Fig. 10). The purpose of the separation is to show that as the applied field \rightarrow zero, $\beta(E) \rightarrow -\alpha_3$, so that at zero applied field the intercept of the Richardson plot is determined by

$$Ue^{-(\epsilon/k)(\alpha_1+\alpha_2)}.$$

To simplify the analysis, the low work function patches are assumed to control the variation of the intercept with activation and applied field. (The approximation is permissible for two reasons: first, that most of the emission comes from the low work function patches, and second, that the work function of these patches is more sensitive to concentration difference and applied field because the patch field above it is a retarding field. The accelerating patch field on the high work function patch introduces only the normal Schottky correction which is small compared with the contribution to the work function of the retarding patch field.)

From Eq. (6), $\gamma(E) + \beta(E)T = \text{increase of work function due to the retarding patch field}$. At zero applied field $\gamma(E) + \beta(E)T = \Delta V/2 = a/2 + bT/2$, from which $\beta(E) = b/2$.

α_3 is the change of work function per degree

change of temperature due to the decrease of concentration in the low work function patches. The temperature dependent part of $\Delta V (= a + bT)$ is a result both of the increase of work function of the low work function patch and of the decrease of work function of the high work function patch when adsorbed atoms pass from the low to the high work function patch. For small changes of concentration, the changes in work function of the two patches may be considered equal. That means that the temperature coefficients of their work functions due to changes in concentration are equal. Since they add up to give the temperature coefficient of ΔV , namely b , then the temperature coefficient of either patch is $b/2$. In particular, the temperature coefficient of the low work function patch with which we are concerned is $b/2$. It has been shown, therefore, that α_3 and $\beta(E)$ are numerically equal at zero applied field. That they have the opposite sign is evident, since an increase in temperature decreases the local fields and therefore their contribution to the work function, while at the same time it decreases the concentration in the low work function patch increasing its work function.

The intercept at zero applied field is, then,

$$Ue^{-(\epsilon/k)(\alpha_1+\alpha_2)}.$$

Since α_1 is not a function of applied field, the variation of the intercept with activation is determined solely by α_2 . From Fig. 7 the low field intercept decreases steadily to a minimum at maximum activity. This requires that α_2 increase steadily with activation to a maximum at maximum activity.

As the applied field is increased from zero, $\beta(E) \rightarrow 0$ due to the neutralization of the local retarding field upon which $\beta(E)$ depends. For applied fields greater than the patch field at the surface, that is, when the local retarding field is completely neutralized, $\beta(E) = 0$. The high field intercept is therefore

$$Ue^{-(\epsilon/k)(\alpha_1+\alpha_2+\alpha_3)}.$$

It differs from the zero field intercept by the additional factor $e^{-(\epsilon/k)\alpha_3}$. It is this factor which shifts the minimum of the high field intercept against activation curve toward $f=0.5$. The argument is as follows: α_3 is the temperature

coefficient of the work function of the low work function patch due to the temperature change of concentration of atoms in the patch. α_3 is large for states of activation up to $f=0.5$, but decreases for activations >0.5 . The reason is the same as that used to explain the variation of ΔV with activation, namely, that a given change of concentration is associated with a larger change of work function at the lower states of activation than at the higher states. α_3 plotted against activation (see Fig. 7) gives a decreasing curve near $f=1$. This added to the curve for $\alpha_1+\alpha_2$ which is increasing slowly to a maximum near $f=1$ shifts the maximum to lower values of f . The maximum of $\alpha_1+\alpha_2+\alpha_3$ corresponds to the minimum in the observed intercept

$$Ue^{-(e/k)(\alpha_1+\alpha_2+\alpha_3)}.$$

7.

The emission lags described in the previous section are *direct evidences* of the *temperature-dependent patch theory*. When the temperature of the filament is dropped from 1600°K to about 1300°K, migration of the atoms at the lower temperature is sufficiently slow to delay the concentration equilibrium from being reached for several minutes. During this time, atoms from the high work function patch migrate to the low work function patch to establish the higher concentration difference characteristic of the lower temperature. Since the low work function patch contributes most of the emission, its decrease of work function with time causes the corresponding increase in the observed emission current. Accompanying changes in the local retarding field have no effect, since the retarding field is neutralized by the high applied field. If, after coming to equilibrium, at the lower temperature, the temperature is suddenly raised to 1600°K, the concentration equilibrium is rapidly established by the greater rate of migration of the atoms, so that no lag effects are observed.

8.

The above observations are for high collecting fields. For low collecting fields, when the temperature is dropped suddenly, the emission is observed to decrease only slightly, if at all, with time. The reason for this is that at low collecting fields changes in the local retarding field above

the low work function patch must be considered as well as changes in the concentration of this patch. The sum of the two effects maintains the emission from the low work function patch constant even though its concentration increases with time. The argument here is the same as that used to show that $\alpha_3 = -\beta(E)$ at low fields, namely, the decrease of work function due to the increase in concentration is equal and opposite to the corresponding increase in work function due to the increased local retarding field. Although the emission from the low work function patch remains constant during the time that the concentration equilibrium is arrived at, the emission from the high work function patch decreases because of its decreasing concentration of atoms. Since the high work function patches account for a small part of the observed emission current, a decrease in its emission will cause the observed slight decrease in the measured current.

9.

Compton and Langmuir¹⁴ report a decrease of the anomalous Schottky effect with increasing temperature. Since, according to the temperature dependent patch theory, the concentration difference approaches zero as the temperature is increased, this observed fact is accounted for quite naturally.

CONCLUSION

The major purpose of this paper will have been satisfied if the temperature dependent patch distribution is established as the most important determinant of the variation of the thermionic constants of thoriated tungsten with applied field and activation. To this end, nine distinct observed facts have been enumerated and analyzed. It is reaffirmed that relatively small effects as surface irregularities and change of effective emitting area with applied field have been neglected to emphasize the more significant aspects of the patch theory. Even with these simplifications the picture is complex. In particular, temperature coefficients of the work function for these surfaces as observed photoelectrically, thermionically and by contact poten-

¹⁴ Compton and Langmuir, *Rev. Mod. Phys.* **2**, 156 (1930).

tial measurement, may not readily be compared before due account is taken of the differences in temperature ranges and applied fields.

The writer is glad to thank Professor L. P. Smith for many helpful discussions on this subject.

APPENDIX

1. Surface factor

The measured emission current from thoriated tungsten is the sum of the emission currents from areas of several different work functions. As such, the Richardson plot of the measured emission current should not be a straight line, since the sum of two exponentials is not an exponential. Actually, the curvature of these plots is not detectable. It has meaning therefore within the experimental accuracy to write

$$I = A_1 T^2 e^{-b_1/T} + A_2 T^2 e^{-b_2/T} = A_3 T^2 e^{-b_3/T}, \quad (1)$$

where I = observed emission current from two patches whose constants are A_1, A_2, b_1 and b_2 while A_3 and b_3 are the observed intercept and slope of a plot of $\ln I - 2 \ln T$ against $1/T$. A_3 may now be calculated in terms of A_1, A_2, b_1 and b_2 to show that its change with applied field due to the increase of $b_2 - b_1$ is much less than the observed change. The variation computed here is the variation of the surface factor $e^{-\delta(B)}$ which has been omitted in the general analysis.

Let $b_2 - b_1 = \Delta b > 0$;
then from (1)

$$I = A_1 T^2 e^{-b_1/T} (1 + A_2/A_1) e^{-\Delta b/T} \quad (2)$$

and $\ln A_3 = \ln I - 2 \ln T + b_3/T$. (3)

From (3): $b_3 = -\frac{d(\ln I - 2 \ln T)}{d(1/T)} = b_1 + \frac{\Delta b}{1 + (A_1/A_2)e^{\Delta b/T}}$. (4)

By inserting $\ln I$ from (2) and b_3 from (4) into (3):

$$\ln A_3 = \ln A_1 + \ln \left(1 + \frac{A_2}{A_1} e^{-\Delta b/T} \right) + \frac{\Delta b}{T(1 + (A_1/A_2)e^{-\Delta b/T})} \quad (5)$$

To get the over-all change of A_3 with applied field due to the change of effective emitting area, let: $A_1 = A_2, b = 2000$ degrees at zero applied field, $T = 1500^\circ\text{K}$. Then from (5)

$$\ln A_3 = \ln A_1 + 0.51. \quad (6)$$

At applied fields greater than the patch field at the surface, $b = 4000$ degrees and

$$\ln A_3 = \ln A_1 + 0.24. \quad (7)$$

From (6) and (7):

$$\frac{A_3 \text{ zero field}}{A_3 \text{ high field}} = 1.3.$$

This change is small compared with the observed change of the order of a factor of 10.

2. Local patch fields

The electrostatic field in the Z direction was computed for the case shown in Fig. 11, where ΔV = contact potential

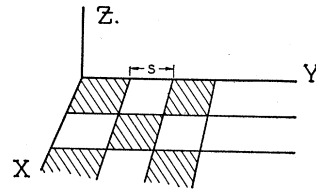


FIG. 11.

difference between the shaded and unshaded square patches and s = length of side of each square. The solution of Laplace's equation

$$\nabla^2 V = 0$$

is $V(x, y, z) = \sum_{\substack{m, n \\ \text{odd}}} \frac{8\Delta V}{mn\pi^2} e^{-(\pi/s)(m^2+n^2)^{1/2}z} \sin \frac{m\pi}{s}x \sin \frac{n\pi}{s}y$,

from which it follows that

$$E_z = \frac{8\Delta V}{\pi s} \sum_{\substack{m, n \\ \text{odd}}} \frac{(m^2+n^2)^{1/2}}{mn} e^{-(\pi/s)(m^2+n^2)^{1/2}z} \sin \frac{m\pi}{s}x \sin \frac{n\pi}{s}y.$$

Using 16 terms of this series gave the field with an accuracy of several percent up to a distance of about 5×10^{-6} cm from the surface.

The low work function patch was divided into sub-squares for each of which the work function was obtained at various applied fields by graphical methods. The work functions of the various sub-squares differed by sufficiently small amounts to allow the arithmetic mean to be taken with an error not greater than 0.02 volt. To average the work functions of the two different kinds of patches, however, the expression obtained above:

$$b_3 = b_1 + \frac{\Delta b}{1 + e^{\Delta b/T}}$$

was used since here Δb was appreciable.